Longitudinal Effects of Symptom Remission on White Matter Microstructure in ADHD

Anne E. M. Leenders[1], Christienne G. Damatac[1,2], Sourena Soheili-Nezhad[1,2], Roselyne J. M. Chauvin[1,2], Maarten J. J. Mennes[1,2], Marcel P. Zwiers[1,2], Daan van Rooij[1,2], Sophie E. A. Akkermans[1,2], Jilly Naaijen[1,2], Barbara Franke[3,4], Jan K. Buitelaar[1,2,5], Christian F. Beckmann[1,2,6], Emma Sprooten[1,2]

[1]Centre for Cognitive Neuroimaging, Donders Institute for Brain, Cognition and Behaviour, Radboud University, Nijmegen, The Netherlands
[2]Department of Cognitive Neuroscience, Donders Institute for Brain, Cognition and Behaviour, Radboud University Medical Centre, Nijmegen, The Netherlands
[3]Department of Human Genetics, Donders Institute for Brain, Cognition and Behaviour, Radboud University Medical Centre, Nijmegen, The Netherlands
[4]Department of Psychiatry, Donders Institute for Brain, Cognition and Behaviour, Radboud University, Nijmegen, The Netherlands
[5]Karakter Child and Adolescent Psychiatry University Centre, Nijmegen, The Netherlands
[6]Centre for Functional MRI of the Brain, University of Oxford, Oxford, UK

To determine the longitudinal effects of symptom dimensions in attention-deficit/hyperactivity disorder (ADHD) on white matter microstructure, we obtained diffusion magnetic resonance imaging (dMRI) data from 99 participants (17-21 years of age, from 65 families) at two time points. Tract Based Spatial Statistics (TBSS) was used to obtain global fractional anisotropy (FA) measures. Effects of symptom dimensions on global FA were analysed using linear mixed-effects models. Permutation-based voxel-wise analyses were performed using Permutation Analysis of Linear Models (PALM). We found that combined symptom dimension score remission is significantly negatively associated with FA at follow-up in the left superior longitudinal fasciculus and the left corticospinal tract (p = .038 and p = .044, respectively). This substantiates earlier findings, where the same effect was shown in an earlier time window within an overlapping cohort. Our results indicate that, in specific white matter (WM) tracts, greater symptom improvement results in less FA at follow-up. We have found no evidence of ADHD-related longitudinal WM alterations at the global brain level.

Keywords: ADHD, white matter microstructure, diffusion MRI, permutation-based TBSS, longitudinal

Corresponding author: Anne E. M. Leenders; E-mail: aemleenders@gmail.com

Attention-deficit/hyperactivity disorder (ADHD) is a common neuropsychiatric disorder characterized by developmentally inappropriate levels of inattention (IA) and/or hyperactivity-impulsivity (HI) with an estimated prevalence of 5% in children and adolescents and 2.5% in adults (Faraone et al., 2015; Polanczyk, Willcutt, Salum, Kieling, & Rohde, 2014). An important source of heterogeneity in the long term outcome of ADHD is the course of the disorder across development. Prospective longitudinal studies suggest that although 15% of people with ADHD continue to meet the full set of diagnostic criteria in adulthood, 60-70% of them retain impairing symptoms of the disorder in adulthood while staying below threshold (Faraone et al., 2015). The question then remains whether there is a particular developmental chronology in the relationship between symptom improvement and changes in the brain. Through the examination of those alterations in relation to disorder progression, we may work towards disentangling the heterogenous nature of ADHD.

Symptom remission can be driven by several neurodevelopmental mechanisms which are neither incompatible nor mutually exclusive. In a remitted individual, symptom improvement may involve brain maturation or normalization, compensation or reorganization, and/or a permanent 'mark' or 'scar' (Sudre, Mangalmurti, & Shaw, 2018). Further, the underlying neural mechanisms that drive symptom remission may generally be dissimilar from those that drive onset. Thus, the brain of an individual with persistent symptoms could be discretely different from the brain of one who has remitted from ADHD (Halperin & Schulz, 2006). The various pathways to remission can be manifest in white matter (WM) microstructure — the foundation of efficient neural communication — and captured longitudinally with diffusion magnetic resonance imaging (dMRI), wherein changes in WM microstructure may be observed as a prediction, concurrence, or product of symptom improvement.

Inherent in the concepts of remission and persistence is the factor of time, underscoring the necessity of longitudinal studies. The upstream, parallel, or downstream development of WM in reference to symptom remission can only be dissected through longitudinal analyses and not through conventional cross-sectional designs. Compared to a cross-sectional approach, a longitudinal design provides not only increased statistical power through reduction of the confounding effect of between-subject variability, but also unique insights into the temporal dynamics of underlying biological processes (Thompson, Hallmayer, & O'Hara, 2011). Between-subject variability is often greater than within-subject differences (i.e., longitudinal effects of interest). Longitudinal studies also reduce within-subject noise and measure within-subject changes directly so that each subject is his/her own control (Reuter, Schmansky, Rosas, & Fischl, 2012). Despite these advantages, a longitudinal dMRI study requires greater attention to methodology in both image processing and statistical modeling.

Past dMRI studies in ADHD have been occluded by a shared set of drawbacks. First, despite the considerable number of studies on the relationship between ADHD and WM microstructure, most are cross-sectional and preclude inferences about the longitudinal trajectory of the disorder. Second, categorical case-control study designs do not account for the continuous nature of ADHD symptoms (van Ewijk et al., 2014). Third, amongst the neural mechanisms that determine the course of a disorder (i.e., symptom remission or persistence), we can make a distinction between moderators and mediators (Baron & Kenny, 1986). Moderators are pre-existing conditions that predict the likelihood of symptoms to remit or persist. Mediators are characteristics whose change over time occurs in parallel to symptom change. A moderator determines when certain effects will take hold, whereas a mediator determines in what way such effects occur. A change in mediating factors is co-occurring and necessary to achieve symptom remission (Baron & Kenny, 1986). The identification of and distinction between moderators and mediators can neither be achieved through traditional case-control designs nor in cross-sectional comparisons of persistent versus remittent ADHD patients, but requires longitudinal investigations.

dMRI studies have related ADHD to abnormalities in WM microstructure, specifically via fractional anisotropy (FA), which is the metric we focus on here (Aoki, Cortese, & Castellanos, 2018; Francx, Oldehinkel, et al., 2015; Shaw et al., 2015; Sudre et al., 2018; van Ewijk, Heslenfeld, Zwiers, Buitelaar, & Oosterlaan, 2012; van Ewijk et al., 2014). dMRI reveals information about anatomical connectivity in the brain in vivo by measuring the directionality of water diffusion in white matter tracts, thus enabling deductions about underlying brain mechanisms through the quantification of associated changes in (inter)cellular space (Beaulieu, 2002; van Ewijk et al., 2014). An FA value of zero indicates fully isotropic diffusion while one indicates fully anisotropic diffusion (Pierpaoli & Basser, 1996). FA is a summary measure of microstructural

integrity that is highly sensitive to myelination. Elevated FA thus represents greater directional coherence of local diffusion (Chang et al., 2017). As it is a computable voxel-wise scalar value that is independent of local WM fiber orientation, FA is a useful quantity to compare across subjects (Smith et al., 2006). A systematic meta-analysis of dMRI studies in individuals with ADHD and typically developing participants found that lower FA in ADHD has mostly been reported in interhemispheric, frontal and temporal regions — however, higher FA has also been found in similar areas (Aoki et al., 2018). Notably, the direction of effects was not consistent across brain regions and studies. The diversity of locations and mixed direction of effects may be caused by differences in sample characteristics, study design and statistical methods (van Ewijk et al., 2012). Consequently, there has been little consensus about the associations of white matter microstructure with different aspects of ADHD such as symptom severity, long-term trajectory, and familiality.

During typical development, WM maturation is greatest during the first few years of life, but myelination continues throughout adulthood, mirrored by differential increases in fractional anisotropy in various brain regions from childhood through adulthood (Dennis & Thompson, 2013). As an ADHD patient develops into adulthood, symptom remission may be underpinned by WM alterations. Not many longitudinal studies have examined the neurobiological underpinnings of symptom remission — and none have included more than one dMRI acquisition. A follow-up dMRI analysis three decades after diagnosis supports the theory of the disorder being an enduring neurobiological trait independent of syndromic remission; Probands had widespread reduced FA compared to those who did not have childhood ADHD (Cortese et al., 2013). Nonetheless, a resting-state functional MRI analysis pointed to the presence of compensatory mechanisms that aid symptomatic remission in prefrontal regions and the executive control network (Francx, Oldehinkel, et al., 2015). The current study aims to longitudinally investigate properties of WM microstructure throughout the trajectory of ADHD. Specifically, we examine changes in FA between two time points and its role in symptom remission. In an overlapping sample from an earlier time window, Francx and colleagues found that less HI symptom remission was associated with more global FA at follow-up in the left corticospinal tract (lCST); They found no association between IA symptom remission and FA (Francx, Zwiers, et al., 2015). While this previous study included clinical data from two time points and only one dMRI time point, our study here is a continuation at a later time window and consists of both clinical and dMRI data from two time points (see Fig. S1 for a graphical representation of how

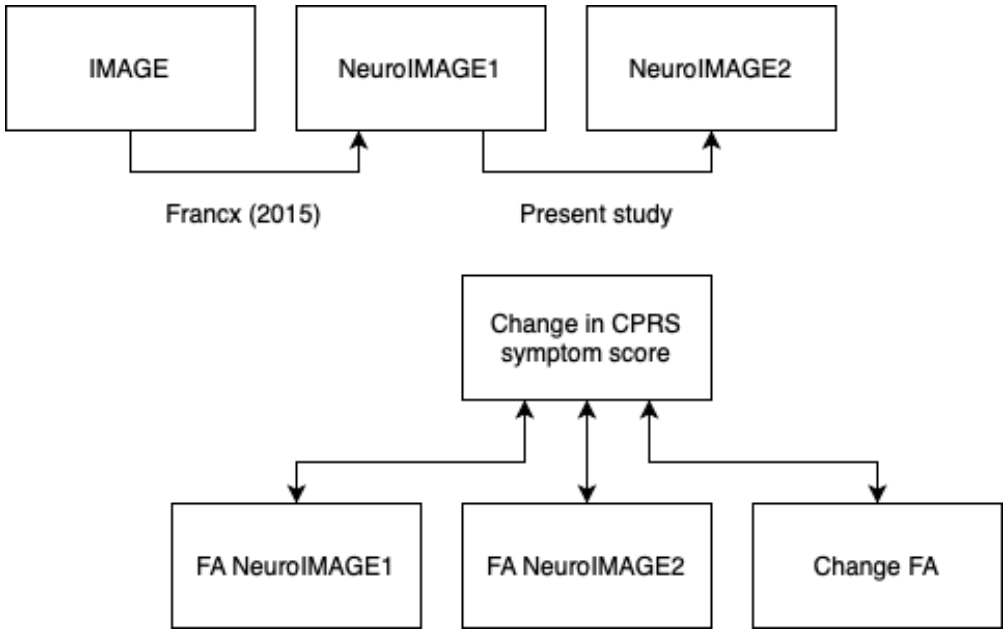

Figure S1. Schematic diagram of the relation of this study to the study of Francx, Zwiers, et al. (2015) (top panel) and a composition of the six different models (bottom panel). Arrows point bi-directionally. Models 1, 2 and 3 have differences in CPRS as the predictor variable. The outcome variables of these models are, respectively, FA TP1, FA TP2 and change in FA. Models 4, and 5 and 6 have the same outcome variable: change in combined CPRS score. Their predictors are respectively FA TP1, FA TP2 and change FA.

our study chronologically relates to that of Francx et al. (2015)).

Recently, in the largest sample to date, we showed that continuous symptom measures of ADHD may be more sensitive to FA than diagnostic categories and that associations of FA with ADHD are not uniformly distributed across WM tracts (Damatac et al., 2020). Against this background, we here employ a dimensional approach with Tract Based Spatial Statistics (TBSS) in a longitudinal fashion to solve issues of cross- and within-subject data alignment, while keeping in mind that ADHD is a complex set of symptoms continuously distributed throughout the population (Smith et al., 2006; Smith et al., 2004). Additionally, we use linear mixed-effects modeling and Permutation Analysis of Linear Models (PALM), a newly available permutation-based analysis technique that restricts permutations to respect family structure in the sample (Winkler, Ridgway, Webster, Smith, & Nichols, 2014; Winkler, Webster, Vidaurre, Nichols, & Smith, 2015). The sample we use is from the NeuroIMAGE cohort including ADHD patients, their unaffected siblings as well as healthy individuals (von Rhein et al., 2015). The project started with a baseline wave (TP0), the International Multicenter ADHD Genetics study (IMAGE), and was followed by two more waves in the Netherlands only, NeuroIMAGE1 (TP1) and NeuroIMAGE2 (TP2). During TP0, only clinical and phenotypic data was collected, various MRI measures started from TP1.

Methods

Participants

Data were collected from probands with childhood ADHD, their first-degree relatives, as well as healthy families (Müller et al., 2011a, 2011b; von Rhein et al., 2015). The current study focused exclusively on individuals that participated in both TP1 and TP2 and have dMRI data available for both time points (N = 120). Individuals with a diagnosis of autism, epilepsy, general learning difficulties, known genetic disorders, brain disorders or IQ < 70 at either time point were excluded. After exclusion for incidental findings, head motion (±3SD), visual quality control, and outliers in global FA (±3SD), the final sample consisted of 99 subjects from 65 families. Normalization of head motion was performed after exclusion of outliers. Global FA at TP1 and TP2, as well as the difference, were normally distributed. Demographic and clinical characteristics of the sample are presented in Table 1.

Clinical measurements

To measure symptom changes over time, semi-structured interviews were conducted using the Conners Parent Rating Scale (CPRS) (Conners et al., 1999) at both TP1 and TP2, assessing the severity of IA and HI symptoms (maximum of 27 per subdomain). The CPRS thus provided us with HI and IA CPRS symptom scores, as well as the combined CPRS symptom score (sum of HI and IA) per subject per time point. Raw CPRS scores were used for this analysis. Symptom change is defined as the difference in CPRS score ($\Delta CPRS = CPRS_{TP1} - CPRS_{TP2}$; thus, symptom improvement is a positive value). IQ was estimated based on WISC or WAIS-III vocabulary and block design subtests at both time points (Wechsler, 2002; Wechsler, 2000).

Data acquisition and pre-processing

Acquisition parameters of the dMRI data are described in detail elsewhere (Damatac et al., 2020; Francx, Oldehinkel et al., 2015). MRI data were acquired with a 1.5 Tesla Siemens Avanto scanner (Siemens Erlangen). The scanner was equipped with an 8-channel phased-array head coil. Whole-brain diffusion-weighted images were collected (twice refocused PGSE EPI; 60 diffusion-weighted directions; b-factor 1000 s/mm^2; 5 non-diffusion weighted images; interleaved slice acquisition; TE/TR = 97/8500 ms; GRAPPA-acceleration 2; phase full Fourier; voxel size 2 x 2 x 2.2 mm).

To minimize movement during acquisition, all participants were trained to keep their head still and received feedback when they moved too much. During pre-processing, the diffusion weightedimages were realigned and corrected for residual eddy current and for artefacts from head and/or cardiac motion using robust tensor modeling (PATCH) (Penny, Friston, Ashburner, Kiebel, & Nichols, 2011; Zwiers, 2010). Head motion is reported in mm frame-wise displacement. All dMRI scans were visually inspected to assess the quality of the data. When the quality was insufficient, data of the subject were excluded (N = 4). Diffusion tensor characteristics, including diffusion eigenvectors, eigenvalues and FA, were calculated for each voxel (Behrens et al., 2003).

Statistical analysis

We performed global FA analyses, followed by voxel-wise analyses. Six mixed-effects models

Table 1. Demographic and clinical characteristics of the sample at the time of dMRI acquisition of NeuroIMAGE1 (TP1) and NeuroIMAGE2 (TP2).

	TP1		TP2		Test Statistic	(P)
	Mean	(SD)	Mean	(SD)		
Age	16.91	(3.47)	20.57	(3.52)		
Sex (female)	42%	N = 42	42%	N = 42		
Estimated IQ*	105.2	(15.02)	106.4	(16.38)	-1.1704	0.2447
Head motion	0.51	(0.25)	0.47	(0.22)	-0.52714	0.5993
Global FA	0.466	(0.02)	0.471	(0.02)	-3.7386	0.0003114
CPRS by group						
Combined	12.76	(12.11)	9.26	(10.20)		
IA	8.05	(7.65)	6.02	(6.65)		
HI	4.71	(5.30)	3.25	(4.23)		

Note. Mean and standard deviation are presented. Combined CPRS symptom score is the sum of two separate subdomains IA and HI.
*Estimated IQ missing for 2 subjects at follow-up.

were composed (Fig. S1). The difference in CPRS symptom score was used as either the predictor (model 1, 2 and 3) or the outcome variable of the models (model 4, 5 and 6). The effects of and on FA at baseline (TP1), follow-up (TP2), and the difference between TP1 and TP2 were tested separately. Fixed effects included gender, normalized head motion at the respective time point, age at TP1, age difference between TP1 and TP2, and CPRS symptom score at TP1. Family was included as a random effect.

Global FA analysis

Global FA was investigated with each of the six models using the package 'lme4' version 1.1-21 in R3.5.1. (Bates, Mächler, Bolker, & Walker, 2015; R Core Team, 2017). In the context of longitudinal dMRI analysis, where within-subject changes are of potentially greater influence than the between-subject changes, we adapted the analysis pipeline according to earlier longitudinal TBSS studies (Engvig et al., 2012; Madhyastha et al., 2014). Longitudinal intra-subject data alignment brings extra difficulty compared to cross-subject nonlinear registration to common space. Intra-subject longitudinal differences are at risk of being removed when different nonlinear warps are used for the same subject at multiple time points. Therefore, using a nonbiased individual subject template has been recommended by Engvig et al. (2012). Madhyastha et al. (2014) provided a script of their pipeline, which is used as the template-pipeline for this study. Figure 1 presents the visualization of this analysis pipeline and the procedure is as follows:

1. Initial registration is a solid automated linear registration using FLIRT with an appropriate optimization schedule validated for accurate longitudinal studies (Jenkinson & Smith, 2001; Smith et al., 2007). Volumes of both time points are resampled into the space halfway between the two (Smith, De Stefano, Jenkinson, & Matthews, 2001), which requires only a single registration per volume, minimizing the registration bias towards one of the time points.

2. The two halfway registered FA-maps are averaged to generate a subject-wise mid-space template (base FA template).

3. A second adaptation of the pipeline smoothens the base FA templates. We added extra mode-dilation and erosion, thus preventing the base FA templates

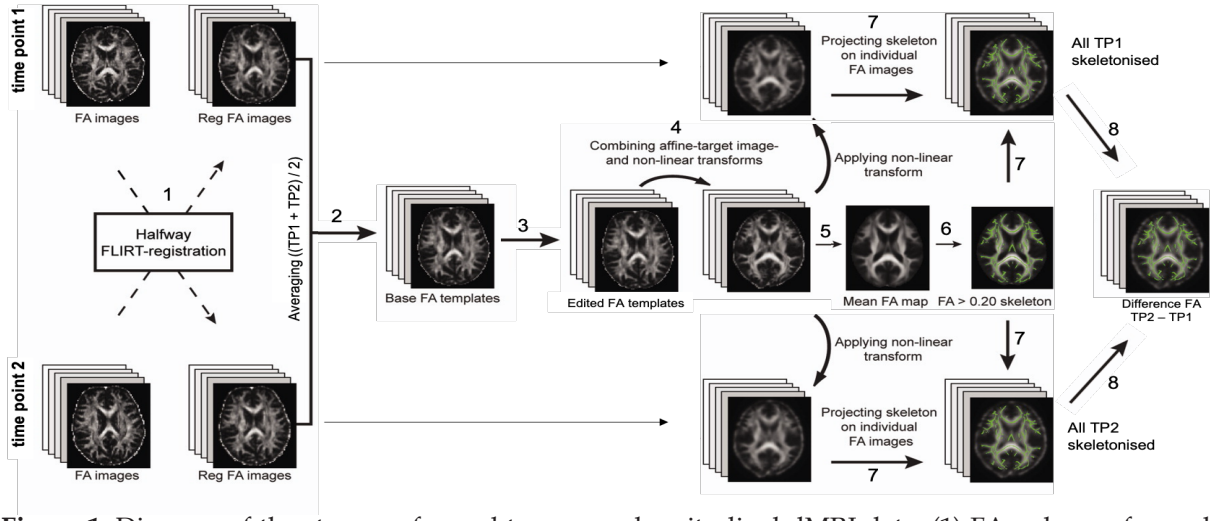

Figure 1. Diagram of the steps performed to process longitudinal dMRI data. (1) FA volumes for each time point for each subject were linearly registered to a space halfway between TP1 and TP2 using FLIRT. (2) From these halfway registered FA volumes, base FA templates were calculated for each subject by averaging the two time points. (3) Then the dilation and erosion took place, (4) and TBSS transformed all smoothened FA images to FMRIB58 FA standard-space. (5) The warped FA templates are used to generate a mean FA map of all subjects and is thinned to create the mean FA skeleton, common to all subjects. (6) The skeleton is thresholded at FA > 0.20 and binarized to reduce the likelihood of partial voluming effects. (7) After warping individual FA volumes to standard space, the mean FA skeleton is projected to the individual volumes for each time point for use in the statistical analyses. (8) Finally, the voxel-wise difference in FA is calculated by subtracting the 4D skeletonised FA images from TP1 from those of TP2.

of inflation of voxels with a value of zero and the disruption of the resultant FA skeleton — giving us an improved, better-connected FA skeleton.

4. TBSS non-linearly registers the base FA template of each subject automatically to FMRIB58 FA standard-space.

5. The mean FA image is created and thinned into a mean FA skeleton, which represents the centers of all tracts common to the sample.

6. The skeleton is thresholded at FA > 0.20 and binarized to suppress areas of low mean FA and/or high inter-subject variability.

7. Aligned FA data of each subject from both time points is projected onto this skeleton.

8. Voxel-wise difference in FA is calculated by subtracting the 4D skeletonised FA images of TP1 from those of TP2.

Voxel-wise analysis

PALM was used to account for the lack of independence in the data due to sibling relationships and shared variance between families; permutation tests between families of the same sizes were constrained (Winkler et al., 2014). In preference for classical permutation methods, we designed multi-level exchangeability blocks which did not allow permutation amongst all individuals; Permutations were constrained both at the whole-block level (i.e., permute between families of the same size) and the within-block level (i.e., permute within families) (Fig. S2). We corrected for multiple testing by running 5000 permutations and threshold free cluster enhancement (TFCE) as implemented in PALM (Smith & Nichols, 2009; Winkler et al., 2014, 2015). The Johns Hopkins University Diffusion Tensor Imaging (DTI)-based white-matter atlas from FSL was used to label white matter tracts (Hua et al., 2008).

We tested three different voxel-wise models. The first model tested for the effect of difference in combined CPRS score on FA at TP1, corrected for gender, head motion at TP1, baseline age, difference in age and baseline combined CPRS score. This is the equivalent of model one for the global FA analysis.

The second voxel-wise model tested for the effect of the difference in combined CPRS score on FA at TP2, corrected for gender, head motion at TP1, baseline age, difference in age and combined CPRS score of TP2. This is the equivalent of model two for the global FA analysis.

The third voxel-wise model tested for the effect of the difference in combined CPRS score on the difference in FA, corrected for gender, head motion at TP1 and TP2, baseline age, difference in age and combined CPRS score of TP2. This is the

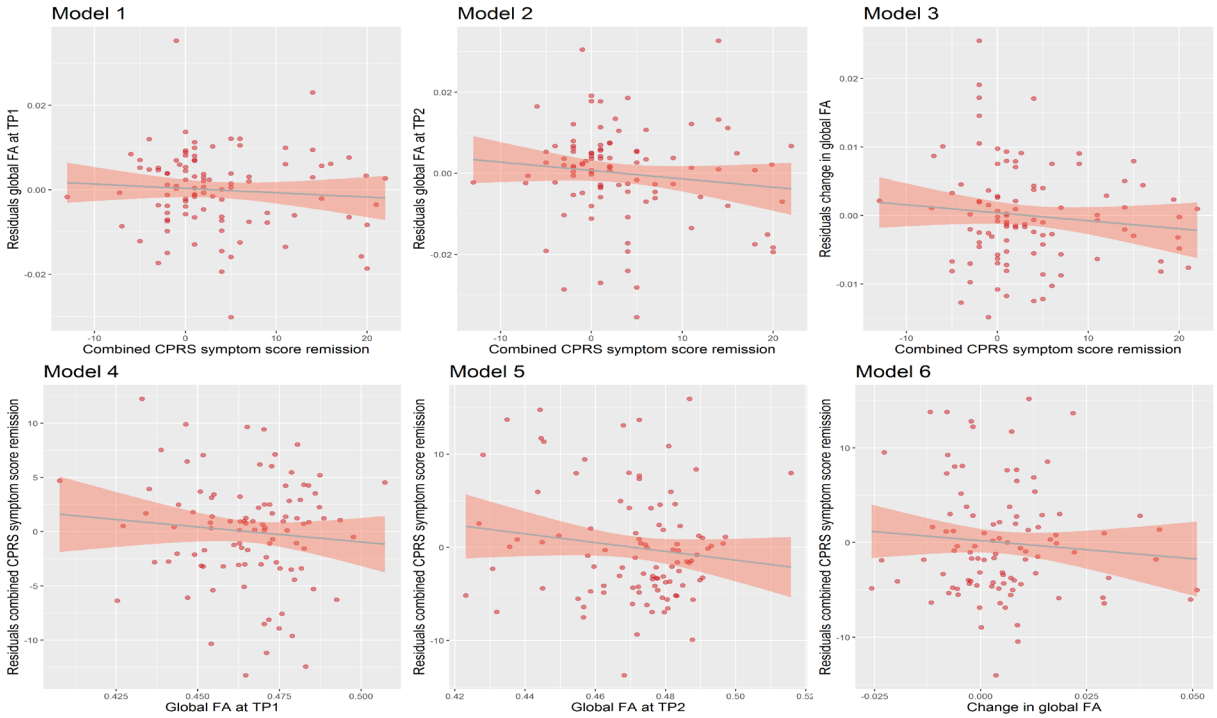

Figure 2. Scatterplots with regression line and 95% confidence interval show the residuals of the linear model of the mixed models without the predictor variable. None of the six models for global FA yielded a significant result (p > .1).

equivalent of model three for the global FA analysis. TFCE corrected $p < .05$ were considered statistically significant. All tests used the standard parameter settings for height, extent and connectivity: H = 2, E = 1, C = 26.

Results

Clinical outcome

Mean symptom scores, separated into the sub scores of HI, IA, and combined (HI + IA) symptom scores, are presented in Table 1. The combined number of symptoms decreased significantly over time ($t(98) = 4.88$, $p < .001$). This was driven by the IA symptom scores ($t(98) = 4.23$, $p < .001$) as well as the HI symptom scores ($t(98) = 4.39$, $p < .001$). Mean decrease in IA symptom domain was 2.04 ($SD = 4.80$), this was 1.46 ($SD = 3.30$) in the HI domain. There was no gender difference in the combined CPRS scores at TP1 ($p = .062$) and at TP2 ($p = .064$). There was no significant difference in the estimated IQ between TP1 and TP2 ($t(97) = -1.17$, $p > .1$).

MRI results

Global FA analysis. Figure 2 presents the outcome of models 1-6. None of the six models for global FA yielded a significant result ($p_{uncorrected} > .1$). Therefore, neither global mean FA at TP1 or TP2 nor the difference in FA showed a significant association with change in ADHD symptom scores ($p_{uncorrected} > .1$). However, all models had effects, though non-significant, in the same direction which could implicate that permutation-based voxel-wise analyses may be more sensitive to location specific results.

Voxel-wise analysis. Model one, two and three were tested in the permutation-based voxel-wise analysis. Model one did not show a significant negative association between combined CPRS symptom score remission and FA at TP1 (Fig. 3A).

Model two resulted in an association for the effect of combined CPRS symptom score remission and FA at TP2. This negative association was found in two different clusters, presented in Table 2. The locations of the clusters are shown in Figure 3B in red; It is the left superior longitudinal fasciculus (lSLF) and the left corticospinal tract (lCST). According to a post-hoc analysis, this negative effect at TP2 is mainly driven by the HI subdomain of the CPRS symptom score; Two clusters are presented in Table 2. The locations of the clusters are shown in Figure 3C in red, mainly located in the lCST.

Model three showed a trend towards a significant negative association between combined CPRS symptom score remission and change in FA ($p = .079$). However, since the effects in model two were mainly driven by the HI domain, a post-hoc

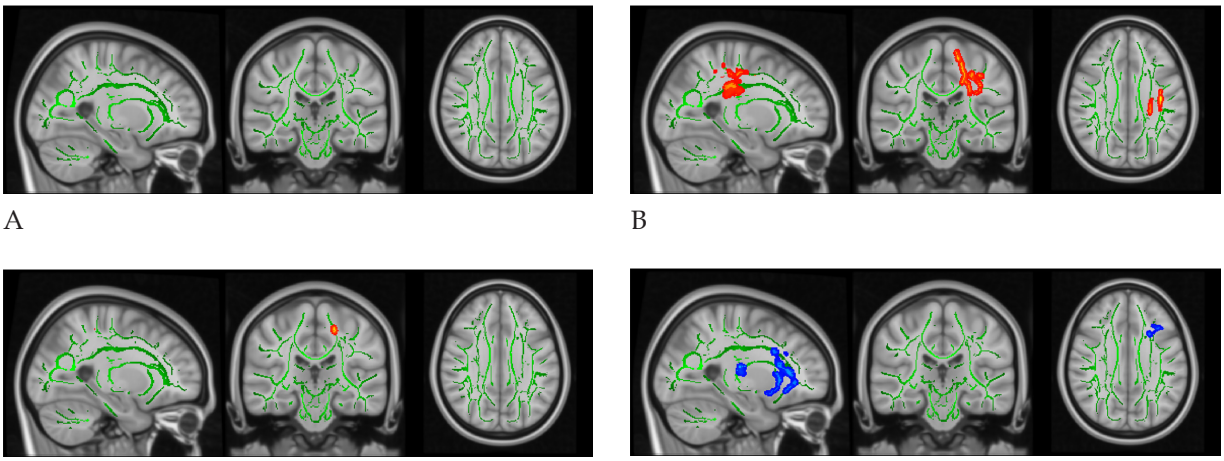

A B C D

Figure 3. Dimensional TBSS analyses showing associations of the effect of combined CPRS symptom remission on FA at the different time points. Mean FA skeleton across all subjects (green) was overlaid on a Montreal Neurological Institute template image for presentation (x = -25, y = -25, z = 31). All associations are in the same direction, different colours are to differentiate between the different models. **A.** Dimensional TBSS analysis showing no significant associations of the effect of combined CPRS symptom remission on FA at TP1. **B.** Dimensional TBSS analysis showing a significant negative association of the effect of combined CPRS symptom remission on FA at TP2 in the left superior longitudinal fasciculus (lSLF) (p = .036) and the left corticospinal tract (lCST) (p = .044). **C.** Dimensional TBSS analysis showing a significant negative association of the effect of the hyperactive/impulsive domain of CPRS symptom remission on FA at TP2 in the left corticospinal tract (lCST) (p = .049). **D.** Dimensional TBSS analysis showing a significant negative association of the effect of the hyperactive/impulsive domain of CPRS symptom remission on the change in FA at several widespread clusters. See Table 2 for the statistics and locations of the clusters.

analysis has been done on the HI subdomain. We found a negative effect of HI on change in FA. More HI symptom remission is thus associated with decreased FA over time. This effect has been found in ten different clusters, mainly in prefrontal parts of the brain. The locations of the clusters are showed in Figure 3D in blue, they are located in the uncinate fasciculus.

Discussion

We did not find a global signdifiature in WM microstructure that can be interpreted as a possible moderator or mediator of remission. However, our results identify more local neural mediators of symptom severity in the longitudinal trajectory of ADHD: Greater combined CPRS symptom remission is significantly associated with less follow-up FA in the lSLF and lCST. This effect is magnified in HI symptom scores, although only in the lCST. These findings are a longitudinal replication of Francx et al. (2015) in the same cohort in a later time window and are partly in line with past reports of ADHD-related alterations in WM microstructure (Francx, Oldehinkel et al., 2015; Onnink et al., 2015; Schweren et al., 2016; van Ewijk

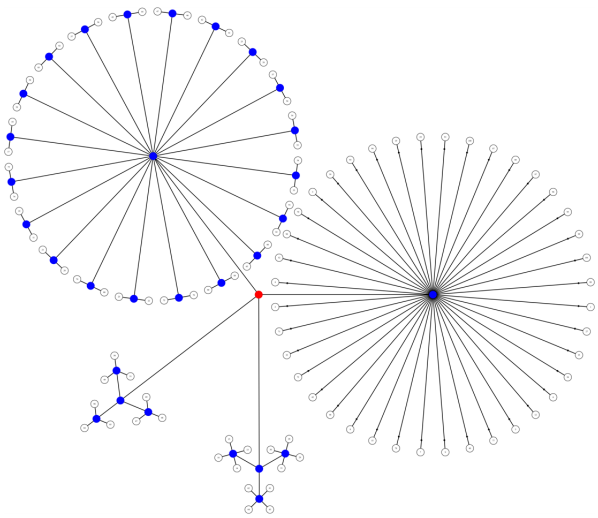

Figure S2. Visual representations for the multi-level notation of the family structure. The four branches represent the size of each family (i.e., three families with four children each). The levels can be depicted as branching from the central red node, akin to a tree in which the most peripheral elements (leaves) represent the observations. The nodes from which the branches depart can be labelled as allowing permutations (blue) or not (red).

et al., 2014). Notwithstanding, given the inclusion of two diagnostic and two dMRI time points, the current study has a more suitable design to detect neural moderators and mediators in ADHD progression. Although a follow-up analysis comes with an increased risk of type I errors and therefore spurious findings, we decided to further examine the HI dimension based on previous investigations that have found, as we did ,that effects of ADHD symptoms on WM microstructure are driven by HI (Damatac, Zwiers, Chauvin, Rooij, & Sophie, 2019; Francx, Oldehinkel et al., 2015; van Ewijk et al., 2012). HI symptom remission may thus be associated with stronger decrease in FA over time.

The longitudinal design here allows us to infer causality: Lower FA in some tracts is a downstream result of symptom remission driven by brain maturation, reorganization, or compensation in other areas, which finally results in less stimulation of those tracts. Others have found the same distinction in persistent and remittent ADHD in various neuroimaging modalities (Clerkin et al., 2013; Francx, Oldehinkel et al., 2015; Francx, Zwiers et al., 2015; Marcos-Vidal et al., 2018; Wetterling et al., 2015). Through the lens of reorganization, lower FA can be attributed to seemingly opposed mechanisms: more axonal sprouting or axonal pruning. Most of the associations we found were clustered in prefrontal regions of the brain. Higher functional connectivity in prefrontal networks in young adults is associated with more improvement in symptoms over time (Clerkin et al., 2013; Francx, Zwiers et al., 2015). Likewise, Halperin and Schulz (2006) hypothesized, based on neuropsychological, imaging and lesion studies, that the prefrontal cortex and its connections are especially important in the persistence of ADHD symptoms. Although several neural factors are known to contribute to the onset of ADHD, they may be largely distinct from those associated with the persistence of symptoms into adulthood (Onnink et al., 2015). As the prefrontal cortex develops, there is potential for it to compensate for the initial causes of ADHD through its connectivity with subcortical regions such as the striatum.

This is not the first time that the SLF and CST have been implicated in ADHD. The SLF generally subserves a wide variety of functions related to language, attention, memory, emotion, and visuospatial function; Many studies have pointed to its function in visuospatial awareness, as well as attentional selection of sensory content (Conner et al., 2018). Here, the effect of overall ADHD symptom change in follow-up SLF FA

Table 2. Peak voxels and localization of significant ($p < .05$) clusters of voxel-wise permutation-based dimensional analyses.

			MNI (Peak voxel)				
	WM	**N Voxels**	**X (COG)**	**Y (COG)**	**Z (COG)**	**t max**	**p value**
FA_TP2 ~ ΔCPRScombined	lCST	723	-21	-27	44	7554	.044
	lSLF	579	-33	-20	38	8810	.038
FA_TP2 ~ ΔCPRSHI	lCST	17	-18	-25	52	9810	.049
FA_Change ~ ΔCPRSHI	lIFOF	508	-29	24	17	4414	.041
	lIFOF	376	-17	31	-10	6127	.035
	Fmin	339	-18	50	0	5854	.042
	lUF	174	-25	17	-8	5635	.045
	lCST	158	-22	-13	8	5624	.047
	Fmin	22	-20	38	21	5629	.049
	CingGyr	17	-17	32	23	5619	.049
	lIFOF	11	-28	15	-1	5627	.049
	Fmin	11	-18	46	17	5659	.049
	Fmin	9	-12	41	-17	5625	.049

Note. MNI, MontrealNeurological Institute; WM, name of the white matter tract; lCST, left cortico-spinal tract; lSLF, left superior longitudinal fasciculus; lIFOF, left inferior fronto-occipital fasciculus; Fmin, forceps minor; lUF, left uncinate fasciculus; CingGy, cingulum (cingulate gyrus).

may be related to the development of attentional selection. A cross-sectional study of response time variability in a sustained attention task found that reduced right SLF FA was associated with a higher frequency of excessively long response times in ADHD participants (Wolfers et al., 2015). The CST integrates cortical and lower brain processing centres in the motor system and has an important role in modulating sensory information, especially in those with ADHD because of the motor hyperactivity that they exhibit (Moreno-López, Olivares-Moreno, Cordero-Erausquin, & Rojas-Piloni, 2016). Altered modulation of sensory information could potentially be involved in HI remission as the CST contains fibers running from the primary motor, premotor, supplementary motor, somatosensory, parietal and cingulate cortex to the spine and, thus, is involved in the control of complex voluntary distal movements (Welniarz, Dusart, & Roze, 2017).

We only found effects locally and exclusively with a dimensional approach. This is in line with recent findings in a large overlapping cohort in which no evidence was found for altered FA in association with categorical ADHD diagnosis (Damatac et al., 2020). Our use of symptom count as a continuous variable maximizes power to detect symptom-related changes, thus presenting a clearer insight into both symptom severity as well as variation in individuals who do not reach diagnostic threshold. Additionally, we utilized more newly developed and suitable techniques with permutation-based voxel-wise analysis, an improved statistical method to correctly account for the family structure in the data (Winkler et al., 2015). Our time window allowed us to investigate both the differences in symptom score and FA over time. Hence, we confirm earlier findings, regardless of the increase in age and even when taking family relatedness more closely into account.

To date, there is no reliable method to predict the likelihood of ADHD remission that could inform treatment options, clinical planning, and lifestyle choices. New hypotheses about prefrontal circuits as mediators in the long-term trajectory of ADHD can be operationalized in animal research and their activity can be experimentally manipulated in human research via techniques such as transcranial magnetic stimulation and neurofeedback (Holtmann, Sonuga-Barke, Cortese, & Brandeis, 2014). These experimental applications could be informative for the development of new treatments, but currently lack evidence-based effective neuroanatomical targets. According to our results, the prefrontal cortex might be an interesting target. Identification of moderators of remission could help the clinical practice in moving towards precision medicine and tailor treatments to individual patients based on their likelihood of remission. Identification of mediating mechanisms of ADHD remission could provide new treatment targets, which are driven by proven mechanisms underlying successful recovery. Our study contributes to the search for neural moderators and mediators.

Conclusion

This is the first time two dMRI time points have been used in a longitudinal study of ADHD. Our results indicate that, in specific WM tracts, greater symptom improvement results in less FA at follow-up. We have found no evidence of ADHD-related longitudinal WM alterations at the global brain level. These findings confirm earlier findings in an overlapping sample and support hypotheses of neural compensation and the role of the prefrontal cortex in the remission of ADHD.

References

Aoki, Y., Cortese, S., & Castellanos, F. X. (2018). Research Review: Diffusion tensor imaging studies of attention-deficit/hyperactivity disorder: meta-analyses and reflections on head motion. *Journal of Child Psychology and Psychiatry*, *59*(3), 193–202.

Baron, R. M., & Kenny, D. A. (1986). The Moderator-Mediator Variable Distinction in Social Psychological Research: Conceptual, Strategic, and Statistical Considerations. *Journal of Personality and Social Psychology*, *51*(6), 1173–1182.

Bates, D., Mächler, M., Bolker, B., & Walker, S. (2015). Fitting Linear Mixed-Effects Models Using {lme4}. *Journal of Statistical Software*, *67*(1), 1–48.

Beaulieu, C. (2002). The basis of anisotropic water diffusion in the nervous system - A technical review. *NMR in Biomedicine*, *15*(7–8), 435–455.

Behrens, T. E. J., Woolrich, M. W., Jenkinson, M., Johansen-Berg, H., Nunes, R. G., Clare, S., … & Smith, S. M. (2003). Characterization and Propagation of Uncertainty in Diffusion-Weighted MR Imaging. *Magnetic Resonance in Medicine*, *50*(5), 1077–1088.

Chang, E. H., Argyelan, M., Aggarwal, M., Chandon, T. S., Karlsgodt, K. H., Mori, S., & Malhotra, A. K. (2017). The role of myelination in measures of white matter integrity: Combination of diffusion tensor imaging and two-photon microscopy of CLARITY intact brains. *NeuroImage*, *147*, 253–261.

Clerkin, S. M., Schulz, K. P., Berwid, O. G., Fan, J., Newcorn, J. H., Tang, C. Y., & Halperin, J. M. (2013). Thalamo-cortical activation and connectivity during response preparation in adults with persistent and

remitted ADHD. *American Journal of Psychiatry*, *170*(9), 1011–1019.

Conner, A. K., Briggs, R. G., Rahimi, M., Sali, G., Baker, C. M., Burks, J. D., … & Sughrue, M. E. (2018). A Connectomic Atlas of the Human Cerebrum—Chapter 10: Tractographic Description of the Superior Longitudinal Fasciculus. *Operative Neurosurgery*, *15*(suppl_1), S407–S422.

Conners, C. K., Erhardt, D., Epstein, J. N., Parker, J. D. A., Sitarenios, G., & Sparrow, E. (1999). Self-ratings of ADHD symptoms in adults I: Factor structure and normative data. *Journal of Attention Disorders*, *3*(3), 141–151.

Cortese, S., Imperati, D., Zhou, J., Proal, E., Klein, R. G., Mannuzza, S., … & Castellanos, F. X. (2013). White matter alterations at 33-year follow-up in adults with childhood attention-deficit/hyperactivity disorder. *Biological Psychiatry*, *74*(8), 591–598.

Damatac, C. G., Chauvin, R. J. M., Zwiers, M. P., van Rooij, D., Akkermans, S. E. A., Naaijen, J., … & Sprooten, E. (2020). White matter microstructure in attention-deficit/hyperactivity disorder: a systematic tractography study in 654 individuals. *BioRxiv*, 787713.

Damatac, C. G., Zwiers, M., Chauvin, R., Rooij, D. Van, & Sophie, E. A. (2019). Hyperactivity-impulsivity in ADHD is associated with white matter microstructure in the cingulum ' s angular bundle, *BioRxiv*, 787713.

Dennis, E. L., & Thompson, P. M. (2013). Typical and atypical brain development: A review of neuroimaging studies. *Dialogues in Clinical Neuroscience*, *15*(3), 359–384.

Engvig, A., Fjell, A. M., Westlye, L. T., Moberget, T., Sundseth, Ø., Larsen, V. A., & Walhovd, K. B. (2012). Memory training impacts short-term changes in aging white matter: A Longitudinal Diffusion Tensor Imaging Study. *Human Brain Mapping*, *33*(10), 2390–2406.

Faraone, S. V, Asherson, P., Banaschewski, T., Biederman, J., Buitelaar, J. K., Ramos-Quiroga, J. A., … & Franke. (2015). Attention-deficit/hyperactivity disorder. *Nature Reviews Disease Primers*, *1*, 1–23.

Francx, W., Oldehinkel, M., Oosterlaan, J., Heslenfeld, D., Hartman, C. A., Hoekstra, P. J., … & Mennes, M. (2015). The executive control network and symptomatic improvement in attention-deficit/hyperactivity disorder. *Cortex*, *73*, 62–72.

Francx, W., Zwiers, M. P., Mennes, M., Oosterlaan, J., Heslenfeld, D., Hoekstra, P. J., … & Buitelaar, J. K. (2015). White matter microstructure and developmental improvement of hyperactive/impulsive symptoms in attention-deficit/hyperactivity disorder. *Journal of Child Psychology and Psychiatry and Allied Disciplines*, *56*(12), 1289–1297.

Halperin, J. M., & Schulz, K. P. (2006). Revisiting the role of the prefrontal cortex in the pathophysiology of attention-deficit/hyperactivity disorder. *Psychological Bulletin*, *132*(4), 560–581.

Holtmann, M., Sonuga-Barke, E., Cortese, S., & Brandeis, D. (2014). Neurofeedback for ADHD: A Review of Current Evidence. *Child and Adolescent Psychiatric Clinics of North America*, *23*(4), 789–806.

Hua, K., Zhang, J., Wakana, S., Jiang, H., Li, X., Reich, D. S., … & Mori, S. (2008). Tract probability maps in stereotaxic spaces: Analyses of white matter anatomy and tract-specific quantification. *NeuroImage*, *39*(1), 336–347.

Jenkinson, M., & Smith, S. (2001). A global optimisation method for robust affine registration of brain images. *Medical Image Analysis*, *5*(2), 143–156.

Madhyastha, T., Mérillat, S., Hirsiger, S., Bezzola, L., Liem, F., Grabowski, T., & Jäncke, L. (2014). Longitudinal reliability of tract-based spatial statistics in diffusion tensor imaging. *Human Brain Mapping*, *35*(9), 4544–4555.

Marcos-Vidal, L., Martínez-García, M., Pretus, C., Garcia-Garcia, D., Martínez, K., Janssen, J., … & Carmona, S. (2018). Local functional connectivity suggests functional immaturity in children with attention-deficit/hyperactivity disorder. *Human Brain Mapping*, *39*(6), 2442–2454.

Moreno-López, Y., Olivares-Moreno, R., Cordero-Erausquin, M., & Rojas-Piloni, G. (2016). Sensorimotor integration by corticospinal system. *Frontiers in Neuroanatomy*, *10*(MAR), 1–6.

Müller, U. C., Asherson, P., Banaschewski, T., Buitelaar, J. K., Ebstein, R. P., Eisenberg, J., … & Steinhausen, H. C. (2011a). The impact of study design and diagnostic approach in a large multi-centre ADHD study: Part 2: Dimensional measures of psychopathology and intelligence. *BMC Psychiatry*, *11*(1), 55.

Müller, U. C., Asherson, P., Banaschewski, T., Buitelaar, J. K., Ebstein, R. P., Eisenberg, J., … & Steinhausen, H. C. (2011b). The impact of study design and diagnostic approach in a large multi-centre ADHD study. Part 1: ADHD symptom patterns. *BMC Psychiatry*, *11*(1), 54.

Onnink, A. M. H., Zwiers, M. P., Hoogman, M., Mostert, J. C., Dammers, J., Kan, C. C., … & Franke, B. (2015). Deviant white matter structure in adults with attention-deficit/hyperactivity disorder points to aberrant myelination and affects neuropsychological performance. *Progress in Neuro-Psychopharmacology and Biological Psychiatry*, *63*(04), 14–22.

Penny, W. D., Friston, K. J., Ashburner, J. T., Kiebel, S. J., & Nichols, T. E. (2011). *Statistical parametric mapping: the analysis of functional brain images*. Elsevier.

Pierpaoli, C., & Basser, P. J. (1996). Toward a quantitative assessment of diffusion anisotropy. *Magnetic Resonance in Medicine*, *36*(6), 893–906.

Polanczyk, G. V., Willcutt, E. G., Salum, G. A., Kieling, C., & Rohde, L. A. (2014). ADHD prevalence estimates across three decades: An updated systematic review and meta-regression analysis. *International Journal of Epidemiology*, *43*(2), 434–442.

R Core Team. (2017). R: A Language and Environment for Statistical Computing. Vienna, Austria. Retrieved from https://www.r-project.org/

Reuter, M., Schmansky, N. N. J., Rosas, H. D., & Fischl, B. (2012). Within-subject template estimation for unbiased longitudinal image analysis. *NeuroImage*,

61(4), 1402–1418.

Schweren, L. J. S., Hartman, C. A., Zwiers, M. P., Heslenfeld, D. J., Franke, B., Oosterlaan, J., … & Hoekstra, P. J. (2016). Stimulant treatment history predicts frontal-striatal structural connectivity in adolescents with attention-deficit/hyperactivity disorder. *European Neuropsychopharmacology*, *26*(4), 674–683.

Shaw, P., Sudre, G., Wharton, A., Weingart, D., Sharp, W., & Sarlls, J. (2015). White matter microstructure and the variable adult outcome of childhood attention deficit hyperactivity disorder. *Neuropsychopharmacology*, *40*(3), 746–754.

Siemens Erlangen. (n.d.). AVANTO.

Smith, S. M., De Stefano, N., Jenkinson, M., & Matthews, P. M. (2001). Normalized accurate measurement of longitudinal brain change. *Journal of Computer Assisted Tomography*, *25*(3), 466–475.

Smith, S. M., Jenkinson, M., Johansen-Berg, H., Rueckert, D., Nichols, T. E., Mackay, C. E., … & Behrens, T. E. J. (2006). Tract-based spatial statistics: Voxelwise analysis of multi-subject diffusion data. *NeuroImage*, *31*(4), 1487–1505.

Smith, S. M., Jenkinson, M., Woolrich, M. W., Beckmann, C. F., Behrens, T. E. J., Johansen-Berg, H., … & Matthews, P. M. (2004). Advances in functional and structural MR image analysis and implementation as FSL. *NeuroImage*, *23*(SUPPL. 1), 208–219.

Smith, S. M., & Nichols, T. E. (2009). Threshold-free cluster enhancement: Addressing problems of smoothing, threshold dependence and localisation in cluster inference. *NeuroImage*, *44*(1), 83–98.

Smith, S. M., Rao, A., De Stefano, N., Jenkinson, M., Schott, J. M., Matthews, P. M., & Fox, N. C. (2007). Longitudinal and cross-sectional analysis of atrophy in Alzheimer's disease: Cross-validation of BSI, SIENA and SIENAX. *NeuroImage*, *36*(4), 1200–1206.

Sudre, G., Mangalmurti, A., & Shaw, P. (2018). Growing out of attention deficit hyperactivity disorder: Insights from the 'remitted' brain. *Neuroscience and Biobehavioral Reviews*, *94*(September), 198–209.

Thompson, W. K., Hallmayer, J., & O'Hara, R. (2011). Design Considerations for Characterizing Psychiatric Trajectories Across the Lifespan: Application to Effects of APOE-ε4 on Cerebral Cortical Thickness in Alzheimer's Disease. *American Journal of Psychiatry*, *168*(9), 894–903.

van Ewijk, H., Heslenfeld, D. J., Zwiers, M. P., Buitelaar, J. K., & Oosterlaan, J. (2012). Diffusion tensor imaging in attention deficit/hyperactivity disorder: A systematic review and meta-analysis. *Neuroscience and Biobehavioral Reviews*, *36*(4), 1093–1106.

van Ewijk, H., Heslenfeld, D. J., Zwiers, M. P., Faraone, S. V., Luman, M., Hartman, C. A., … & Franke, B. (2014). Different mechanisms of white matter abnormalities in attention-deficit/ hyperactivity disorder: A diffusion tensor imaging study. *Journal of the American Academy of Child and Adolescent Psychiatry*, *53*(7), 790-799.e3.

von Rhein, D., Mennes, M., van Ewijk, H., Groenman, A. P., Zwiers, M. P., Oosterlaan, J., … & Buitelaar, J. K. (2015). The NeuroIMAGE study: a prospective phenotypic, cognitive, genetic and MRI study in children with attention-deficit/hyperactivity disorder. Design and descriptives. *European Child and Adolescent Psychiatry*, *24*(3), 265–281.

Wechsler, D. (2002). WISC-III Handleiding. *The Psychological Corporation, London*.

Wechsler, D. (2000). WAIS-III Nederlandstalige bewerking. Technische handleiding. London: The Psychological Corporation.

Welniarz, Q., Dusart, I., & Roze, E. (2017). The corticospinal tract: Evolution, development, and human disorders. *Developmental Neurobiology*, *77*(7), 810–829.

Wetterling, F., Mccarthy, H., Tozzi, L., Skokauskas, N., O'Doherty, J. P., Mulligan, A., … & Frodl, T. (2015). Impaired reward processing in the human prefrontal cortex distinguishes between persistent and remittent attention deficit hyperactivity disorder. *Human Brain Mapping*, *36*(11), 4648–4663.

Winkler, A. M., Ridgway, G. R., Webster, M. A., Smith, S. M., & Nichols, T. E. (2014). Permutation inference for the general linear model. *NeuroImage*, *92*, 381–397.

Winkler, A. M., Webster, M. A., Vidaurre, D., Nichols, T. E., & Smith, S. M. (2015). Multi-level block permutation. *NeuroImage*, *123*, 253–268.

Wolfers, T., Onnink, A. M. H., Zwiers, M. P., Arias Vasquez, A., Hoogman, M., Mostert, J. C., … & Franke, B. (2015). Lower white matter microstructure in the superior longitudinal fasciculus is associated with increased response time variability in adults with attention- deficit/hyperactivity disorder. *Journal of Psychiatry & Neuroscience*, *40*(5), 344–351.

Zwiers, M. P. (2010). NeuroImage Patching cardiac and head motion artefacts in diffusion-weighted images. *NeuroImage*, *53*(2), 565–575.